

Electronic density of states of amorphous Si and Ge: Application of a molecular-liquid model

N. C. Halder

Department of Physics, University of South Florida, Tampa, Florida 33620

(Received 25 April 1979)

The electronic structures of *a*-Si and *a*-Ge have been investigated by introducing the molecular-liquid model (MLM). The theoretical structure factors have been expressed in terms of three simple parameters—nearest-neighbor distance, packing density, and coordination number. For the electronic density of states (EDS), nonlocal energy-dependent pseudopotentials have been considered to second order in perturbation theory. When compared with the experimental structure factors, the MLM structure factors agree well for the momentum transfer in the region of $0 < k < 4 \text{ \AA}^{-1}$, but there is some departure for higher values of k . The calculated energy values exhibit a number of new features in the E_2 vs k curves that were not noticed previously with local-pseudopotential and on-Fermi-surface approximation. The EDS, however, show remarkably good agreement with recent theoretical and experimental results.

I. INTRODUCTION

In this paper we will report our investigation on the electronic density of states (EDS) of amorphous silicon (*a*-Si) and amorphous germanium (*a*-Ge) by introducing two new concepts: (i) a molecular-liquid model¹⁻³ (MLM) to derive the structure of *a*-Si and *a*-Ge; and (ii) a nonlocal energy-dependent pseudopotential⁴⁻⁶ to calculate the EDS. Previously we have published⁷ the results of EDS for *a*-Si and *a*-Ge, where experimentally obtained spherically symmetric interference functions (structure factors) were used, along with the local pseudopotential under on-Fermi-surface (OFS) approximation. The results of that study⁷ were semiquantitative and, as a consequence, there was a noticeable difference between our results and other available theoretical results. The present investigation is an attempt, as will be shown later in this paper, to treat the problem more comprehensively and appropriately with an aim to find a greater quantitative agreement with other theories and experiments which have recently appeared in the literature.

II. BRIEF REVIEW OF PROGRESS IN THE FIELD

We shall briefly review the highlights of the progress already made in this direction. There have been a large number of publications⁸ on amorphous semiconductors, but we shall restrict ourselves only to those which are specifically relevant to the present work.

A. Electronic density-of-states techniques

For the discussion of EDS we may conveniently select four major techniques which seemingly have received the greatest popularity and, in most part,

have enjoyed relative success. These are the linear-combination-of-atomic-orbitals (LCAO) approach, tight-binding approach, Green's-function approach, and the perturbation approach.

The LCAO method, also known as the extended Huckel theory, was started by Bloch, but a thorough discussion of this method is given by Slater and Koster.⁹ This method has been adopted by many workers¹⁰⁻¹² to obtain EDS in amorphous semiconductors, and some reasonably good results have been obtained. Very recently another version of this technique, known as the linear combination of bond orbitals, has been suggested¹³ for amorphous semiconductors.

Weaire and his co-workers¹⁴ developed a simple tight-binding approach for calculating the EDS of *a*-Si and *a*-Ge. They assumed that a topologically disordered Hamiltonian could be used in this type of calculation. An array of identical potentials which are not periodically positioned is said to be positionally disordered. Weaire and Thorpe¹⁴ found that the electronic properties of solids are dominated by the short-range order (SRO). It is only the theory that is dominated by long-range order (LRO) because of the convenience of the Bloch theorem. This theory is not compatible with the existence of localized states throughout the gap.

Vanderbauwhede and Phariseau¹⁵ have used the tight-binding approach to calculate EDS in another fashion. They introduced the concept of the paracrystal and the complex paracrystal. The well-known radial distribution function (RDF) may then be replaced by a more appropriate distance statistic. This allows the details of the SRO and angular correlations to be introduced into the calculation.

Henderson and Ortenburger¹⁶ have used a tight-binding model for the electronic structure of amorphous solids. Although they considered polytypes

of Si and Ge with only 8 and 12 atoms in a unit cell (the Si-III and Ge-III structures, respectively), the results were in fair agreement with the experimental values.^{17,18} The Ge-III structure was found to be a plausible approximation to the structure of *a*-Ge. It accounts for the main features of the RDF, EDS, and the optical properties of *a*-Ge, although not much can be said for the quantitative results of these calculations.

The Green's-function approach has been worked out for amorphous solids by Kramer.¹⁹ Subsequently he¹⁹ has calculated the EDS in *a*-Si and *a*-Ge using a generalized pseudopotential formalism based on the Green's-function technique. This technique also gives results which are qualitatively, or at best semiquantitatively, in agreement with the experiment, but detailed fitting of the experimental data was not attempted. Gubanov²⁰ also used the Green's-function approach to calculate the electron density in the band tail of amorphous semiconductors. His calculations have been criticized. For instance, Spicer, Donovan, and Fisher¹⁸ have considered the evidence for band tails and have determined that the thin films prepared in the manner described in their work, i.e., the sample density being 98% of the crystalline value, do not have states in the gap; no evidence of band tailing was found. The existence of band tails has now been associated with voids and impurities in the sample rather than with the positional disorder. In general, the Green's-function technique leads to a smaller secular equation than other calculational methods. However, the matrix elements which must be evaluated are generally more complicated, each structure factor involving a long summation over exponential functions, spherical harmonics, and integrals which must be evaluated numerically. Calculations done by the Green's-function method generally require as much computer time as those done by the tight-binding method.

One of the modifications of the Green's-function method is the cluster approach suggested by Keller.²¹ Keller²¹ has shown that one could include the cluster of different size, shape, and geometry to calculate EDS of amorphous semiconductors, especially *a*-Si and *a*-Ge. Ziman²² has worked out the Green's-function perturbation theory for polycrystalline and amorphous solids with SRO necessary to explain the observed band gaps. He²² shows that by adjusting the orientations of SRO and assuming a cluster of as large as five atoms, but without any LRO, one could alternatively interpret the results of EDS. Cohen and Bergstresser²⁸ have studied the band properties of Si and Ge using pseudopotentials. This has been extended by Joannopoulos and Cohen²⁸ to investigate EDS. Many

OPW treatment of the properties of Si with pseudopotential theory has met with reasonable success.²³

B. Modeling of structure of amorphous semiconductors

Many attempts²⁴⁻³² have been made at modeling the structure of amorphous semiconductors. All these models have one thing in common—they all make use of the information in the coordinate space, such as bond lengths, bond angles, coordination numbers, ring statistics, dihedral angle distributions, and deviations from the regular tetrahedral network. However, our model, as will be explained in Sec. III, will involve information from the reciprocal space. Let us first briefly describe some of the important developments in model building.

1. Expanded-crystal model

Herman and Van Dyke³³ calculated EDS under the assumption that the amorphous material would be nearly 30% less dense than the crystalline phase. This assumption was based on the experimental results of Clark,³⁴ who used samples prepared by ordinary evaporation techniques not under the stringent conditions mentioned previously. Herman and Van Dyke³³ calculated the crystalline density of states with a larger atomic spacing to allow for the lower density. This calculation led to semimetal conduction and was obviously not satisfactory. The expanded-crystal model, as mentioned above, was abandoned; it is now almost universally accepted⁸ that the structure of *a*-Si and *a*-Ge is a random tetrahedral network.

2. Microcrystal model

In this model²⁴⁻²⁶ one approaches the amorphous structure by taking a collection of atoms of about 10–20 Å in size with random orientations of these microcrystals. This consideration, however, would imply many more “dangling bonds” than would be necessary to describe the actual amorphous state. Furthermore, a particular type of random crystal model of *a*-Si has also been ruled out owing to substantial experimental disagreements.

3. Perturbed-crystal model

One of the ways this model²⁷ can be tested is to try a set of calculations on the computer. In this approach the atoms are arranged alternately on three crystalline polymorphs sites of Si with positions varied by a Monte Carlo procedure; the final arrangement, which gives the closest agreement with the expected RDF and the structure factor, is retained. In a similar spirit some calculations of the states of *a*-Si and *a*-Ge have been done by Joannopoulos and Cohen²⁸ and others²⁹ by introduc-

ing larger and larger atomic cells with various relative positions of the tetrahedrally bonded atoms attached to each atomic site. In this approach the unchanged features of the EDS are interpreted as arising from the tetrahedral coordination, i.e., SRO rather than LRO. Kramer¹⁹ and Unger³⁰ have considered crystalline lattices with randomly disordered atoms positioned according to Gaussian distributions about their mean crystal-line sites.

4. Continuous-random-network model

The structure of amorphous solids in the continuous-random-network model (CRM)^{31,32,35} is constructed from an infinite nonperiodic three-dimensional array of atoms. The SRO is then incorporated by chemical bonding requirements, i.e., the atoms must be tetrahedrally bonded, appropriate bond angles and bond lengths must be retained, etc. In this type of network each atom is linked to its four nearest neighbors. The central atom and its four nearest neighbors form a distorted tetrahedron. The tetrahedral bonds are randomly oriented with respect to each other. The orientations range from the extreme eclipsed to the staggered configuration. Under these conditions the first two peaks of the RDF of the amorphous solid are retained, while the third peak is missing. This is in agreement with experimental results. This model is by far the best model, since it produces most of the essential features of the actual amorphous structure. However, this model does not yield an analytical expression for the structure in a closed or iterative form, which should be useful, sometimes even required, for many other calculations.

III. MOLECULAR-LIQUID-MODEL STRUCTURE FACTORS

One of the aims of our present approach is to suggest another form for the structure, one that does not depend on a finite-size system or on any underlying LRO existing directly or in the zero disorder limit. The model should incorporate, however, most or all of the insights provided by the CRM. The structure factor $I(q)$ obtained from experimental measurements³⁶⁻³⁸ unquestionably indicates that $I(q)$ is intermediate between the crystalline form (sharp δ -function-like peaks at reciprocal lattice points) and the liquid form (similar to the Percus-Yevick³⁹ expression) of the same density. This evidence suggests a parameterization of the structure in terms of the MLM of the same density with the molecules of the system consisting of clusters of tetrahedrally bonded atoms. Interpreted in coordinate space, the proposed model will have the characteristics shown in Fig. 1. The parameters of the distorted tetra-

hedral unit are to be selected in concurrence with the chemical bonding requirement of the solid. The size of the SRO sphere will indicate the amount of amorphicity in the otherwise totally disordered solid.

We consider the atomic structure factor of a system consisting of N atoms,⁷

$$I(q) = \frac{1}{N} \sum_{i,j} \langle e^{i\vec{q} \cdot \vec{r}_{ij}} \rangle, \quad (3.1)$$

where \vec{r}_{ij} represents the atomic positions and $\langle \rangle$ denotes a statistical averaging over all such positions for the given interaction between the atoms. We treat the atoms as being bound in clusters of $Z+1$ atoms, one reference atom being surrounded by Z atoms. We now denote the molecular positions by $l=1, 2, \dots, N/(Z+1)$ and atomic ones by $\alpha=0, 1, 2, \dots, Z$. Thus we may write

$$\vec{r}_{l\alpha} = \vec{R}_l + \vec{\rho}_{l\alpha}, \quad (3.2)$$

where \vec{R}_l is the position of the l th molecule, and $\vec{\rho}_{l\alpha}$ is that of the α th atom, with respect to the reference atom which is positioned at $\alpha=0$. From Eq. (3.1) we obtain, therefore,

$$I(q) = \frac{1}{N} \sum_{l=1}^{N/(Z+1)} \left\langle e^{i\vec{q} \cdot \vec{R}_l} \sum_{\alpha=0}^Z e^{i\vec{q} \cdot \vec{\rho}_{\alpha l}} \right\rangle. \quad (3.3)$$

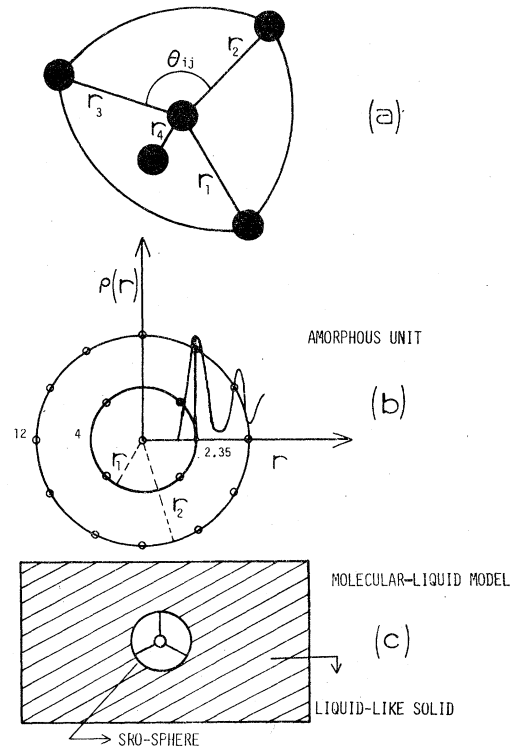


FIG. 1. Proposed model for amorphous semiconductors. (a) Distorted tetrahedral unit, (b) molecular unit, (c) amorphous solid.

One has to give the random variables \vec{R}_i and $\vec{\rho}_{i\alpha}$ the weighting effect appropriate to the CRM that is presently computed³² numerically. Since the exact weighting functions are not known analytically, some physically relevant correlations must be introduced to achieve our goal. These points have been discussed elsewhere.⁴⁰

We have purposely split the correlations in the amorphous structure into two parts: (i) a strong SRO correlation within a cluster or molecule with the positions or orientations of atoms specified within a narrow range as in a solid; and (ii) a weak LRO analogous to a liquidlike correlation between the molecules themselves. The essential advantage is that the two correlations are being separately treated.

With a set of realistic approximations it is now possible to obtain an expression for the structure factor as a product of two terms:

$$I(q) = S_L(q)S_T(q), \quad (3.4)$$

where $I(\infty) \approx 1$, true for amorphous solid, liquid, and gas. The respective structure factors may be completely written^{39,40}

$$S_T(q) = 1 + Zj_0(qa) + Z \left(j_2(qa) - \frac{j_1(qa)}{qa} \right) \left(\frac{q\sigma_p}{qa} \right)^2 \quad (3.5)$$

and

$$S_L^{-1}(q) = 1 + \frac{24\eta}{(1-\eta)^4} \left[(1+2\eta)^2 (C_0 + \frac{1}{2}\eta C_2) - 6\eta(1 + \frac{1}{2}\eta)^2 C_1 \right], \quad (3.6)$$

where

$$x = 2qR_0, \quad (3.7)$$

$$C_0 = \left(\frac{s}{x^2} - \frac{c}{x} \right) / x, \quad (3.8)$$

$$C_1 = \left[2s - \frac{2}{x} + \left(\frac{2}{x} - x \right) c \right] / x^3, \quad (3.8)$$

and

$$C_2 = (4s - xc) / x^3 - 12C_1 / x^2. \quad (3.9)$$

In the above equations σ_p is the variable radial disorder parameter so that σ_p/a is usually very small, j_l is the spherical Bessel function, $s = \sin x$, and $c = \cos x$. The packing density function η is obtained from

$$\eta = \pi\rho_0(2R_0)^3/6(Z+1), \quad (3.10)$$

where ρ_0 is the atomic density appropriate to the temperature and semiconductor. In the present investigation, $0 < \eta < 0.63$ and the radius of the molecular (cluster) sphere R_0 are treated as a free parameter. In the CRM the requirement that the network be continuous really cuts down the available space for relative rotation and displacement of the clusters. We expect, therefore, that

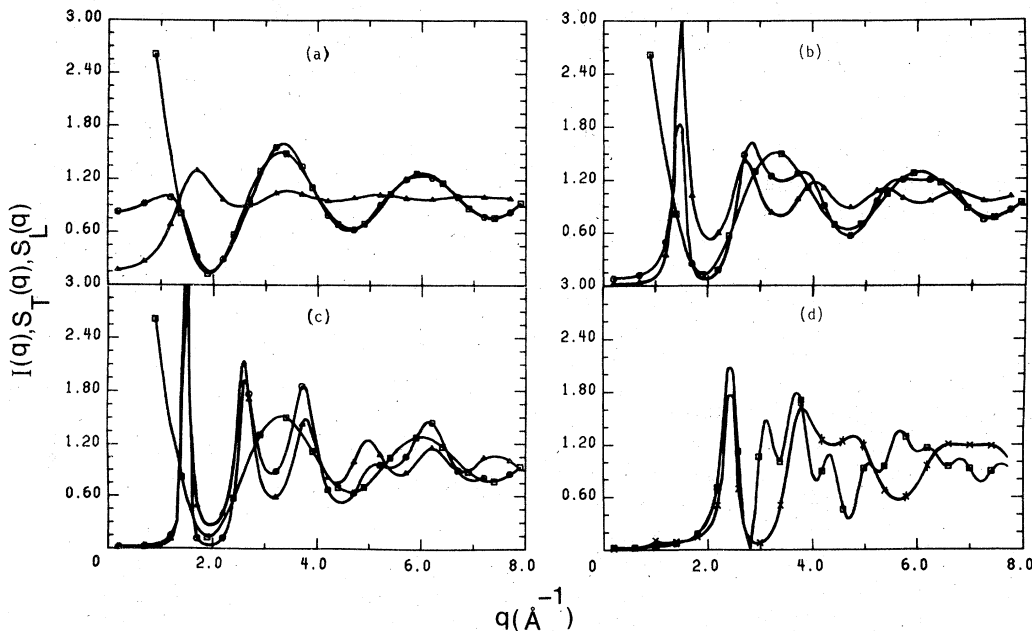


FIG. 2. The plots of $S_L(q)$, $S_T(q)$, and $I(q)$ for α -Si are shown in (a), (b), and (c) for packing densities $\eta = 0.23$, 0.50 , and 0.63 , respectively. \square : $S_T(q)$, Δ : $S_L(q)$, and \circ : $I(q)$. (d) The plot of MLM $I(q)$, after correction for angular correlation, is shown along with experimental (Ref. 36) $I(q)$ for α -Si. \times : MLM $I(q)$ and \square : experimental $I(q)$.

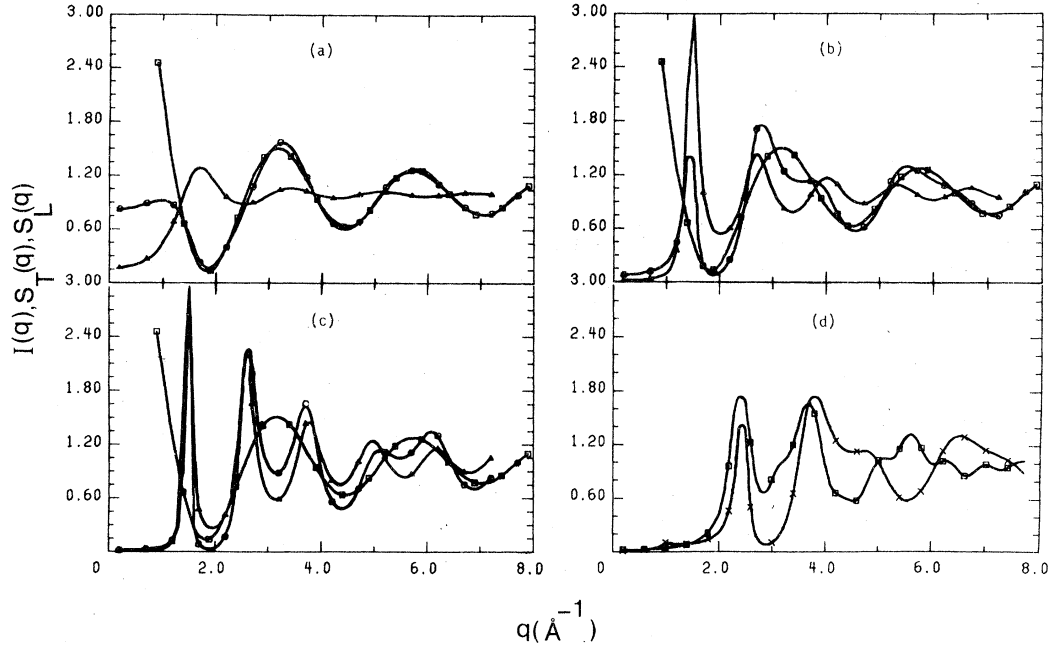


FIG. 3. The plots of $S_L(q)$, $S_T(q)$, and $I(q)$ for a -Ge are shown in (a), (b), and (c) for packing densities $\eta=0.23$, 0.50 , and 0.63 , respectively. \square : $S_T(q)$, Δ : $S_L(q)$, and \circ : $I(q)$. (d) The plot of MLM $I(q)$, after correction for angular correlation, is shown along with experimental (Ref. 37) $I(q)$ for a -Ge. \times : MLM $I(q)$ and \square : experimental $I(q)$.

the effect of this reduction of available space will be seen in the MLM approach by a molecular radius larger than that of a sphere enclosing all the atoms.

In Figs. 2 and 3 we show the plots of $S_L(q)$, $S_T(q)$, and $I(q)$ for $\eta=0.23$, 0.50 , and 0.63 , with $a=2.35$ Å. These are obtained with a set of physical parameters shown in Table I. The plots corresponding to $\eta=0.50$ seem to be more realistic when compared with direct experimental data. In Figs. 2(d) and 3(d) are shown the MLM $I(q)$, along with the corresponding experimental $I(q)$. It should be noted, however, that these MLM $I(q)$ have been corrected for angular correlations as mentioned for free molecular rotations. We have done so somewhat semiquantitatively by introducing a "shift parameter." This means that the computed plots of Figs. 2(c) and 3(c) are shifted to the right by $\Delta q = 1.0$ Å⁻¹ to match with the first peak maximum of the experimental $I(q)$. The net effect of the shift parameter is to incorporate empirically the numerical difference that is introduced in consideration of the free rotation of the clusters with respect to one another. At present no exact calculation is available to remedy this situation any more quantitatively than we have suggested here.

The plots with packing density $\eta=0.50$ show the best agreement with experiments. The intermolecular structure factor $S_L(q)$ varies rather rapidly with the increase of q . In the region of small q ,

$S_T(q)$ strongly dominates over $S_L(q)$. The first minimum in $I(q)$ is due primarily to the effect of the valley of $S_T(q)$ which overcomes the first peak in $S_L(q)$. The small deviations observed between the MLM $I(q)$ and experimental^{36,37} $I(q)$ beyond the second peak maximum could arise from the two different viewpoints with regard to normalization procedure used in the experimental $I(q)$. It is generally assumed in the experimental work that the diffracted intensity of x-ray or electron experiment from a -Si and a -Ge at large values of q (>5 Å⁻¹) is due primarily to the total independent scattering, i.e., equal to the square of the atomic structure factor $\langle f \rangle^2$. This is what is done for

TABLE I. Physical parameters for Si and Ge.

Parameters	Si	Ge
Density	2.33 g/cm ³	5.36 g/cm ³
Melting temperature	1420°C	958.5°C
Atomic weight	28.09	72.59
Atomic number	14	32
Coordination number	4	4
Atomic configuration	3s ² 3p ²	4s ² 4p ²
Lattice parameter	5.430 Å	5.658 Å
Nearest-neighbor distance	2.35 Å	2.45 Å
Radius of atom	1.17 Å	1.22 Å
Band energy gap at 23°C	1.11 eV	0.78 eV
Fermi energy	12.51 eV	11.56 eV

atomic solids; but for molecular solids, as we are suggesting for α -Si and α -Ge, this factor should be $5\langle f \rangle^2$. Probably in the reported experimental works^{36,37} this difference was not realized. It is quite likely that more experimental measurements with appropriate normalization constants will be the source of the final answer. Nevertheless, what is demonstrated here is that $I(q)$ in the physically relevant region is caused by a coupling between the intermolecular and intramolecular correlations. The first-order approximations considered here give results of $I(q)$ that are physically meaningful and acceptable. One could, however, improve the agreement by using the recent developments in the theory of molecular liquids.

IV. BAND ENERGIES OF AMORPHOUS SOLIDS

In the spirit of the Animalu-Heine⁴ model potential we may consider the ionic potential as a sum of local and nonlocal parts,

$$w(r) = w_L(r) + w_N(r), \quad (4.1)$$

where the matrix elements of the potential may be correspondingly expressed⁶ as

$$w(E, q, \vec{k}, \vec{k}') = w_L(E, q, \vec{k}, \vec{k}') + w_N(E, q, \vec{k}, \vec{k}'). \quad (4.2)$$

In previous works⁴¹ the nonlocal part was not considered significant and has been neglected for the

sake of mathematical simplicity. We shall, of course, have to replace the bare ion matrix element $w_i(E, q, \vec{k}, \vec{k}')$ by the screened matrix element $w_i^s(E, q, \vec{k}, \vec{k}')$. We show in Figs. 4 and 5 the individual components $w_N(E, q, \vec{k}, \vec{k}')$, $w_N^e(E, q, \vec{k}, \vec{k}')$, and nonlocal correction term $w_N^s(E, q, \vec{k}, \vec{k}')$ at the Fermi energy. The contrasting sign of the function $w_N^s(E, q, \vec{k}, \vec{k}')$ for α -Si and α -Ge should be noted, however, especially in the region of low momentum. This occurs because of the different weighting effect caused by the spectroscopic parameters A_i , which are not identical for the two solids.

In accordance with second-order perturbation theory, we may write the electron energy as

$$E(k) = E_0(k) + E_1(k) + E_2(k), \quad (4.3)$$

where

$$E_0(k) = (\hbar^2/2m)k^2, \quad (4.4)$$

$$E_1(k) = E_1^L(k) + E_1^N(k), \quad (4.5)$$

and

$$E_2(k) = E_2^L(k) + E_2^{LN}(k) + E_2^N(k). \quad (4.6)$$

In these equations the superscripts L and N denote, respectively, the contributions from the local and nonlocal terms of the models. The various energy terms can be written in terms of the appropriate matrix elements w_i^s of the screened model potentials. While the details of these cal-

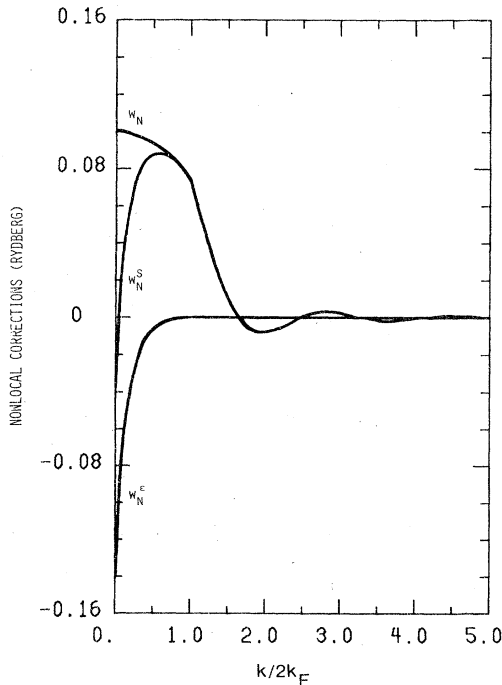


FIG. 4. The plots of the model potential matrix elements for Si at the Fermi energy.

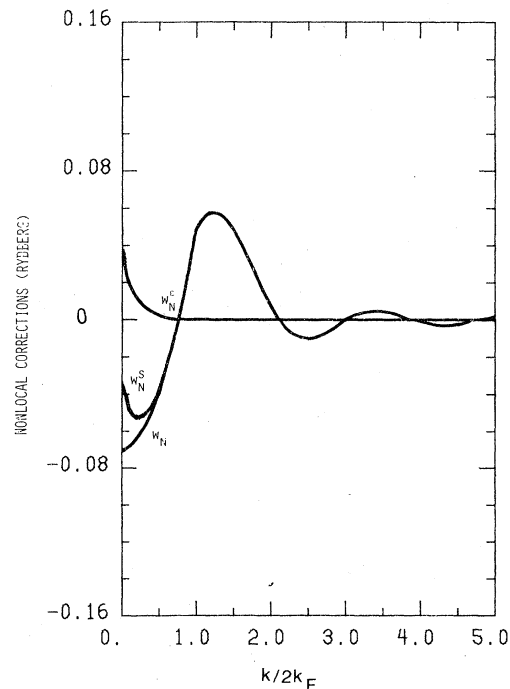


FIG. 5. The plots of the model potential matrix elements for Ge at the Fermi energy.

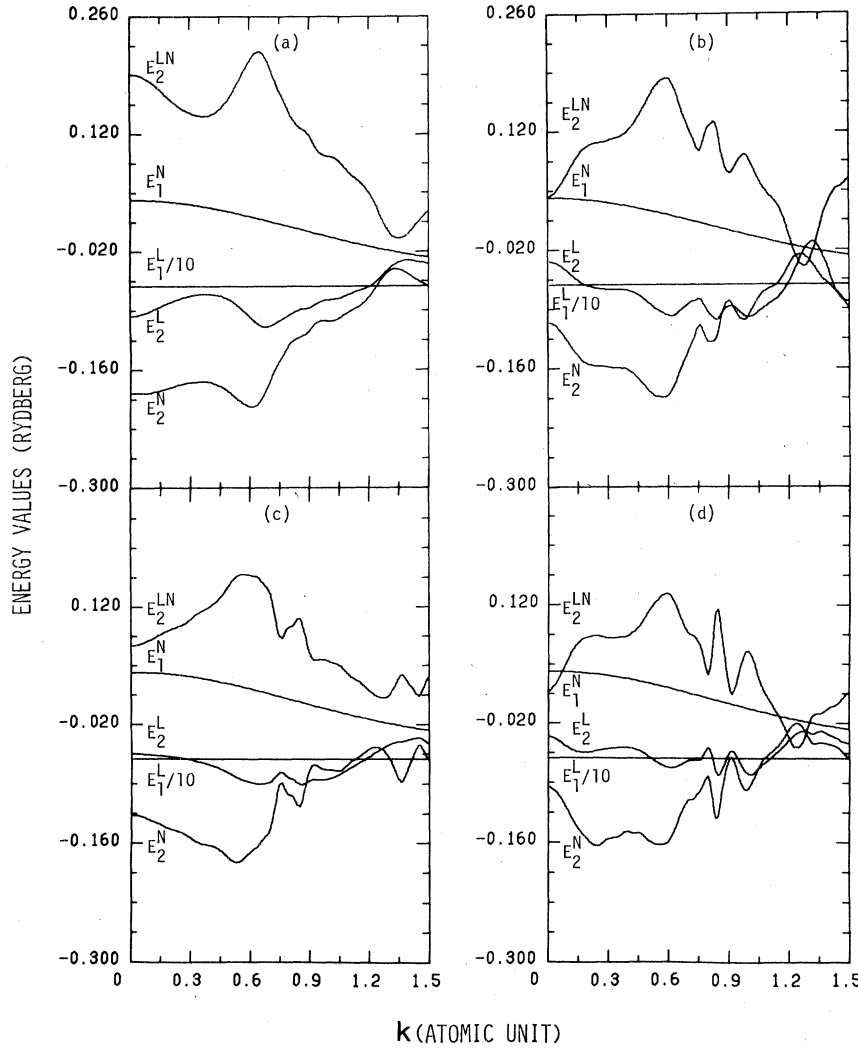


FIG. 6. The plots of the various energy values for Si. (a) Hard-sphere liquid (Ref. 40) Si, (b) experimental (Ref. 36) *a*-Si, (c) Henderson-Herman (Ref. 17) *a*-Si, and (d) present MLM *a*-Si.

culations can be found elsewhere,⁴² we summarize the essential points for the sake of self-consistency and completeness. Thus,

$$E_1^L(k) = w_L^s(E, 0, \vec{k}, \vec{k}), \quad (4.7)$$

$$E_1^N(k) = w_N^s(E, 0, \vec{k}, \vec{k}), \quad (4.8)$$

and

$$E_2^{ij}(k) = \frac{\Omega_0}{(2\pi)^3} c_{ij} \times \int d\vec{q} \frac{-I(q) w_i^s(E, q, \vec{k}, \vec{k}') w_j^s(E, q, \vec{k}, \vec{k}')}{q^2 + 2kq \cos \theta_{\vec{k}\vec{k}'}} \quad (4.9)$$

where $c_{ij} = 1$ for $i = j$, but $c_{ij} = 2$ for $i \neq j$. The expanded forms of these equations have been obtained⁴² by utilizing the model potential parameters, where provision has been made for the energy dependence.

The computed plots of all the energy terms for

a-Si are displayed in Fig. 6 and for *a*-Ge in Fig. 7. Except for the first-order energy terms $E_1^L(k)$ and $E_1^N(k)$, all other terms show a number of important features. These features strongly reflect the modulations in the MLM $I(q)$. The first-order terms, $E_1^L(k)$ and $E_1^N(k)$, do not contain the $I(q)$ term and, therefore, are devoid of these features. The energy values adequately satisfy the requirement of convergence of the perturbation series in that they show $E_0(k) > E_1(k) > E_2(k)$.

V. ELECTRON DENSITY OF STATES

The EDS expression, in terms of the free-electron density of states $g_0(E)$, may now be written

$$\frac{g(E)}{g_0(E)} = \frac{2k^3}{\pi^2} \left(2k + \frac{\partial E_1^N(k)}{\partial k} + \frac{\partial E_2^L(k)}{\partial k} + \frac{\partial E_2^N(k)}{\partial k} + \frac{\partial E_2^L(k)}{\partial k} + \frac{\partial E_2^N(k)}{\partial k} \right)^{-1}. \quad (5.1)$$

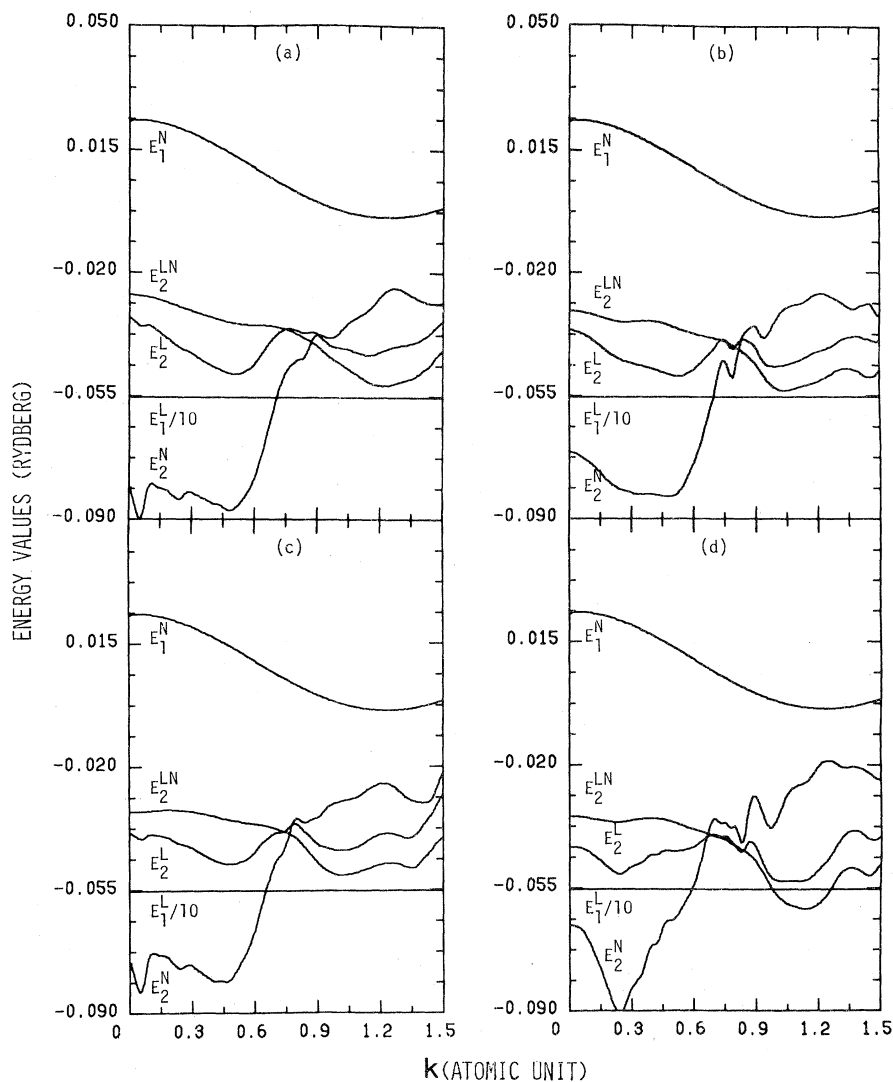


FIG. 7. The plots of the various energy values for Ge. (a) Hard-sphere liquid (Ref. 40) Ge, (b) experimental (Ref. 37) α -Ge, (c) Henderson-Herman (Ref. 17) α -Ge, and (d) present MLM α -Ge.

Equation (5.1) is more detailed than what we proposed in our earlier work⁷ for local pseudopotential with OFS approximation. Since there is no k -dependent parameter in $E_1^L(k)$, it does not contribute anything to the EDS. Furthermore, except for $\partial E_1^N(k)/\partial k$, there does not seem to appear any other analytic form. All these calculations are, therefore, performed numerically. The EDS plots for α -Si and α -Ge are shown in Figs. 8 and 9. The zero of the energy scale was chosen at the Fermi level. As expected, on the positive side of the energy scale only the conduction band should be positioned, and hence not much feature is observed. However, on the negative side of energy we notice splitting of the valence band owing to $3s$ and $3p$ electrons of α -Si, and $4s$ and $4p$ electrons of α -Ge. Furthermore, some additional features, owing to the effect of all the core bands,

are also observable.

Our results of EDS may be directly compared with some recent theoretical^{19,28,43,44} and experimental^{17,18,45-51} results. The important point is that the present results for both α -Si and α -Ge [see Figs. 8(d) and 9(d)] may be examined with (i) the Green's-function calculation of Kramer,¹⁹ (ii) the LCAO calculation of Choo and Tong,⁴³ and (iii) the dynamical-matrix (DM) calculation of Meek.⁴⁴ All the essential features of EDS plots are retained, even better than LCAO and DM calculations to some extent. This is perhaps a significant achievement.

VI. SUMMARY AND CONCLUSIONS

For the energy values the dominating term in all cases is the first-order local term $E_1^L(k)$. The

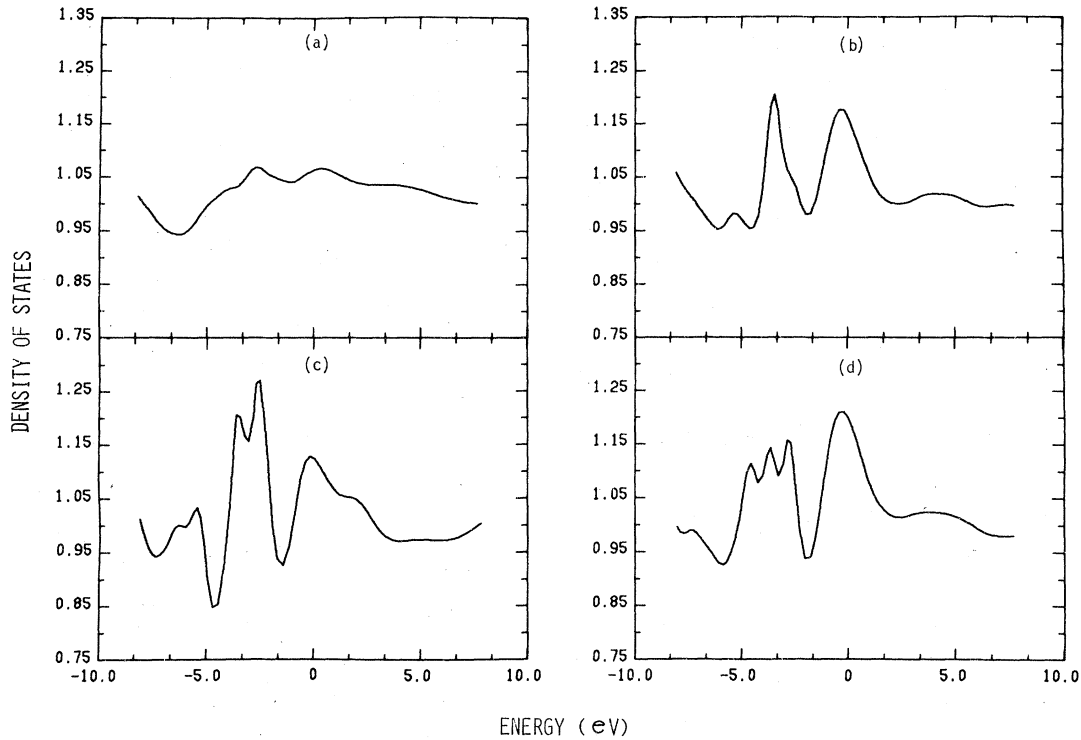


FIG. 8. The plots of EDS for Si. In these plots EDS have been expressed in units of free-electron density of states $g_0(E)$, and the Fermi energy is scaled to zero. (a) Hard-sphere liquid Si, (b) experimental a -Si, (c) Henderson-Herman a -Si, (d) present MLM a -Si.

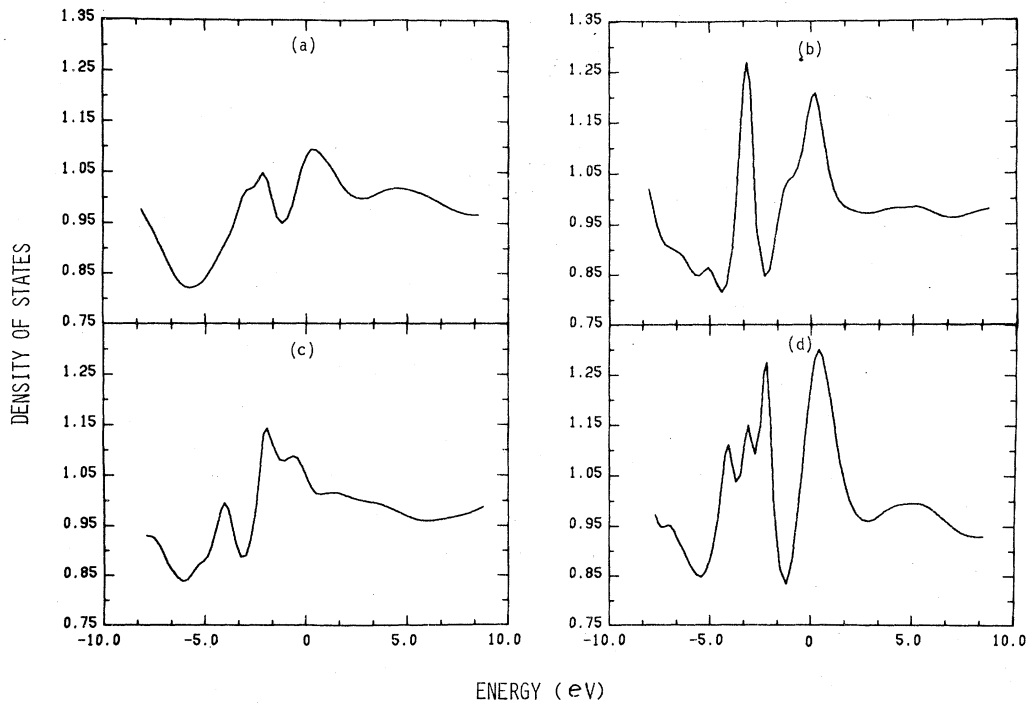


FIG. 9. The plots of EDS for Ge. In these plots EDS have been expressed in units of free-electron density of states $g_0(E)$, and the Fermi energy is scaled to zero. (a) Hard-sphere liquid Ge, (b) experimental a -Ge, (c) Henderson-Herman a -Ge, (d) present MLM a -Ge.

variation of the $E_1^N(k)$ term is relatively smooth. The pronounced oscillatory behavior of $E_2^L(k)$, $E_2^N(k)$, and the cross term $E_2^{LN}(k)$ gives very sharp derivatives, which enter automatically into the calculation of the EDS. It is the effect of this sharpness that determines the shapes of EDS plots. As pointed out before, through the discussion of nonlocal matrix elements in Figs. 4 and 5, the nonlocal part $w_N^s(E, q, \vec{k}, \vec{k}')$ is positive for Si and negative for Ge in the region of low momentum. This effect is felt in the cross term $E_2^{LN}(k)$, meaning thereby that its sign is always positive for α -Si, but negative for α -Ge. The other terms, however, are not changed in sign owing to the presence of quadratic form in the energy integrand of Eq. (4.9). The energy values of the second-order terms are relatively higher for α -Si than those for α -Ge. This picture is consistent with our expectations from the model potential parameters themselves. The features of liquid Si and liquid Ge, as observed in Figs. 6(a) and 7(a), have the least number of kinks, which serves as an indication of a uniformly disordered system. As we gradually put more order in the system, more kinks (or better, kinky behavior) begin to grow both in number and in intensity. These effects, in turn, influence the EDS plots.

The plots in Figs. 8 and 9 show systematically how the structural effects change the characteristics of EDS. For liquid⁴¹ Si and Ge, as seen from the plots in Figs. 8(a) and 9(a), the EDS are almost featureless. On the other hand, EDS obtained with experimental^{36,37} $I(q)$ and MLM $I(q)$ are quite close to one another. This is self evident from Figs. 8(b), 8(d), 9(b), and 9(d) for both α -Si and α -Ge. The Henderson-Herman¹⁶ model is also used for calculation of EDS. The general features of EDS, as demonstrated by Figs. 8(d) and 9(d), are qualitatively correct when compared with other theoretical results.^{43,44} These plots bring out for the first time a consistent picture of the relationship between the structure and the EDS of amorphous solids and liquidlike solids.

McGill and Klima⁵² have also developed a method of calculating EDS, assuming that the atoms of α -Si and α -Ge are clustered in groups of eight in tetrahedral bonding in the staggered or eclipsed configuration. This results in two RDF's. The curves are very similar, suggesting that the ener-

gy gap for the amorphous solid should be very nearly equal to that of the corresponding crystal. Cohen *et al.*⁵³ have suggested that in certain amorphous semiconductors, EDS's have an overlap; the conduction and valence bands have tails of localized states sufficiently extensive to overlap near the center of the mobility gap. An alternate model, suggested by Mott and Davis,⁵⁴ has a fairly narrow band of localized states (less than 0.1 eV) near the center of the gap. However, recent evidence indicates that, if the Polk density conditions are met, there are no states in the center of the gap. It is suspected that previously observed states could be due to unsatisfied bonds, interstitials, etc., which vary with preparation methods and other experimental conditions.

We now concentrate on the band positions in Figs. 8(d) and 9(d) in comparison with Green's-function calculations. For α -Si the peaks at -2.85 , -3.64 , -4.56 , and -7.25 eV and for α -Ge the peaks at -2.18 , -3.11 , -4.07 , and -6.93 eV agree remarkably well with the sp -hybridized peaks reported by Kramer.¹⁹ However, these peaks seem to lose most of their identity in their corresponding liquid states. The presence of the dips around -5.86 eV for α -Si and around -5.45 eV for α -Ge are also in good agreement with the LCAO and Green's-function calculations. The cluster of these peaks in the valence band is due primarily to the hybridization of s - and p -like bands. It has already been recognized⁴³ that the positions of the dip and, we might add, the resolution of the peaks in the valence-band cluster would strongly depend on the strain in the bond and bond angles of the distorted tetrahedral unit. In our case it would include all the physical parameters of the molecular unit of Fig. 1.

Finally, in summarizing, we may point out that the MLM structure factors, together with the nonlocal energy-dependent pseudopotentials, can explain the atomic and electronic structure of α -Si and α -Ge. These results do predict the correct band gaps and band positions as they have been observed by LCAO and Green's-function methods. The local pseudopotentials with OFS approximation are somewhat less quantitative for EDS calculations. It would probably be worthwhile to study more complicated systems with the present approach with some modifications.

¹P. A. Egelstaff, *An Introduction to the Liquid State* (Academic, New York, 1967).

²C. J. Pings, *Physics of Simple Liquids*, edited by H. N. V. Temperley, J. S. Rowlinson, and G. S. Rushbrooke (Wiley, New York, 1968), p. 389.

³L. J. Lowdon and D. Chandler, *J. Chem. Phys.* **61**, 5228 (1974).

⁴A. O. E. Animalu and V. Heine, *Philos. Mag.* **12**, 1249 (1965); A. O. E. Animalu, *ibid.* **11**, 379 (1965).

⁵W. A. Harrison, *Pseudopotentials in the Theory of*

- Metals* (Benjamin, New York, 1966).
- ⁶S. R. Shenoy and N. C. Halder, *Phys. Rev. B* 11, 690 (1975); D. Y. Kuan, S. R. Shenoy, and N. C. Halder, *ibid.* 16, 1735 (1977).
- ⁷N. C. Halder and R. L. Wourms, *Z. Naturforsch.* 30a, 55 (1975); N. C. Halder, *The Properties of Liquid Metals*, edited by S. Takeuchi (Taylor and Francis, London, 1972).
- ⁸See, for example, *Physics of Structurally Disordered Solids*, edited by S. S. Mitra (Plenum, New York, 1976).
- ⁹J. C. Slater and G. F. Koster, *Phys. Rev.* 94, 1498 (1954).
- ¹⁰R. P. Messmer and G. D. Watkins, *Phys. Rev. B* 7, 2568 (1973).
- ¹¹B. Y. Tong, J. R. Swenson, and F. C. Choo, *Phys. Rev. B* 10, 3338 (1974); F. C. Choo, B. Y. Tong, and J. R. Swenson, *Phys. Lett. A* 50, 764 (1974).
- ¹²G. G. Hall, *Philos. Mag.* 43, 338 (1952); 3, 429 (1958).
- ¹³J. M. Ziman, *J. Phys. C* 4, 3129 (1971).
- ¹⁴D. Weaire, *Phys. Rev. Lett.* 26, 1541 (1971); D. Weaire and M. F. Thorpe, *Phys. Rev. B* 4, 2508 (1971); M. Thorpe and D. Weaire, *Phys. Rev. Lett.* 27, 1581 (1971).
- ¹⁵A. Vanderbauwhede and P. Pahiseau, *Physica (Utrecht)* 51, 561 (1971).
- ¹⁶D. Henderson and F. Herman, *J. Non-Cryst. Solids* 8-10, 359 (1972); D. Henderson and I. Ortenburger, *Computational Solid State Physics* (Plenum, New York, 1972).
- ¹⁷T. M. Donovan and W. E. Spicer, *Phys. Rev. Lett.* 21, 1572 (1969); T. M. Donovan, W. E. Spicer, and J. M. Benett, *ibid.* 22, 1058 (1969).
- ¹⁸W. E. Spicer and T. M. Donovan, *J. Non-Cryst. Solids* 2, 66 (1970); W. E. Spicer, T. M. Donovan, and J. E. Fisher, *ibid.* 8-10, 122 (1970); D. T. Pierce and W. E. Spicer, *Phys. Rev. B* 5, 3017 (1972).
- ¹⁹B. Kramer, *Phys. Status Solidi B* 41, 649 (1970); 47, 501 (1971).
- ²⁰A. I. Gubanov, *Quantum Electron Theory of Amorphous Conductors* (Consultants Bureau, New York, 1965).
- ²¹J. Keller, *J. Phys. C* 4, 3143 (1971).
- ²²J. M. Ziman, *J. Phys. C* 2, 1704 (1969); *Proc. R. Soc. London A* 318, 1535 (1970).
- ²³D. Brust, *Phys. Rev.* 134, A1337 (1964).
- ²⁴R. Grigorovici and J. Manaila, *Nature (London)* 226, 143 (1970).
- ²⁵M. V. Coleman and D. J. D. Thomas, *Phys. Status Solidi* 22, 593 (1970); 24, K111 (1968).
- ²⁶Y. F. Tsay, D. K. Paul, and S. S. Mitra, *Phys. Rev. B* 8, 2827 (1973).
- ²⁷R. Kaplow, T. A. Rowe, and B. L. Averbach, *Phys. Rev.* 168, 1068 (1968).
- ²⁸J. D. Joannopoulos and M. L. Cohen, *Solid State Phys.* 31, 71 (1976); *Phys. Rev. B* 7, 2644 (1973); *Phys. Rev.* 8, 2733 (1973); T. K. Bergstresser and M. L. Cohen, *ibid.* 164, 1069 (1967); M. L. Cohen and T. K. Bergstresser, *ibid.* 141, 798 (1969).
- ²⁹G. A. N. Connell and R. J. Tempkin, *Tetrahedrally Bonded Amorphous Semiconductors*, edited by M. H. Brodsky, S. Kirkpatrick, and D. Weaire (American Institute of Physics, New York, 1974), p. 192; W. Paul and G. A. N. Connell, *Physics of Disordered Solids*, edited by S. S. Mitra (Plenum, New York, 1974), p. 45.
- ³⁰H. J. Unger, *Phys. Status Solidi B* 76, 207 (1976); 76, 841 (1976).
- ³¹R. Grigorovici and J. Manaila, *J. Non-Cryst. Solids* 1, 371 (1969).
- ³²D. E. Polk, *J. Non-Cryst. Solids* 6, 365 (1971); D. E. Polk and D. S. Bourdreaux, *Phys. Rev. Lett.* 31, 92 (1973).
- ³³F. Herman and J. P. Van Dyke, *Phys. Rev. Lett.* 21, 1575 (1968).
- ³⁴A. H. Clark, *Phys. Rev.* 154, 750 (1967).
- ³⁵N. J. Shevchik and W. Paul, *J. Non-Cryst. Solids* 8-10, 381 (1971).
- ³⁶S. C. Moss and J. F. Graczyk, *Proceedings of the Tenth International Conference on the Physics of Semiconductors* (U.S. AEC, Oak Ridge, Tenn., 1970), p. 658.
- ³⁷H. Richter and G. Breitling, *Z. Naturforsch. Teil A* 13, 988 (1958); 18, 23 (1963).
- ³⁸M. H. Brodsky, R. S. Title, K. Wiser, and G. D. Pettit, *Phys. Rev. B* 1, 2632 (1970).
- ³⁹N. W. Ashcroft and J. Lekner, *Phys. Rev.* 145, 83 (1966).
- ⁴⁰N. C. Halder and S. R. Shenoy, *J. Non-Cryst. Solids* (to be published).
- ⁴¹P. Jena and N. C. Halder, *Phys. Rev. B* 6, 2131 (1972); N. C. Halder and P. Jena, *J. Chem. Phys.* 57, 1830 (1972).
- ⁴²N. C. Halder, *Phys. Rev. B* (to be published).
- ⁴³F. C. Choo and B. Y. Tong, *Structure and Excitations of Amorphous Solids*, edited by G. Lucovsky and F. L. Galeener (American Institute of Physics, New York, 1976), Vol. 31, p. 58.
- ⁴⁴P. E. Meek, *Philos. Mag.* 33, 897 (1976); *J. Phys. C* 10, L59 (1977).
- ⁴⁵L. Ley, S. Kowalczyk, R. Pollak, and D. A. Shirley, *Phys. Rev. Lett.* 29, 1088 (1972).
- ⁴⁶V. G. Aleshin and Y. N. Kucherenko, *Bull. Acad. Sci. USSR, Phys. Ser.* 40, 80 (1976); *J. Electron Spectrosc. Relat. Phenom.* 8, 411 (1976).
- ⁴⁷M. L. Rudee and A. Howie, *Philos. Mag.* 25, 1001 (1972).
- ⁴⁸M. L. Theye, *Physics of Structurally Disordered Solids*, edited by S. S. Mitra (Plenum, New York, 1974), p. 111.
- ⁴⁹W. D. Grobman and D. E. Eastman, *Phys. Rev. Lett.* 29, 1508 (1972).
- ⁵⁰G. A. N. Connell, *Solid State Commun.* 14, 377 (1974).
- ⁵¹D. Engemann and R. Fisher, *Phys. Status Solidi B* 79, 195 (1977).
- ⁵²T. C. McGill and J. Klima, *J. Phys. C* 3, L163 (1970); *Phys. Rev. B* 5, 1517 (1972).
- ⁵³M. H. Cohen, H. Fritzsche, and S. R. Ovshinsky, *Phys. Rev. Lett.* 22, 1065 (1969).
- ⁵⁴N. F. Mott and E. A. Davis, *Electronic Processes in Non-Crystalline Materials* (Clarendon, Oxford, 1971).